How to Model Solvation of Peptides? Insights from a Quantum Mechanical and Molecular Dynamics Study of *N*-Methylacetamide. 2. ^{15}N and ^{17}O Nuclear Shielding in Water and in Acetone

Benedetta Mennucci*,† and José M. Martínez‡

Dipartimento di Chimica e Chimica Industriale, Università di Pisa, via Risorgimento 35, 56126 Pisa, Italy, and Departamento de Química Física, Universidad de Sevilla, Facultad de Química, Sevilla 41012, Spain

Received: January 4, 2005; In Final Form: March 10, 2005

This paper represents the second part of a study of solvation of peptides. As in the first part, *N*-methyl acetamide has been used to model the specific features of solvation of the peptide linkage. In this part of the study, devoted to nuclear magnetic shieldings, acetone and water have been used as examples of polar and/or hydrogen-bond donor/acceptor solvents. Once again, three different solvation models have been tested and compared, namely, a continuum only description, a discrete description in terms of solute−solvent clusters, and a mixed discrete/continuum description in terms of clusters embedded in a continuum. Both QM and classical simulation (e.g., MD) approaches have been used to determine the structure of the clusters. The analysis of the results of the three different models, when combined with those obtained in the first part of the study devoted to IR and UV spectra, has allowed us to identify and characterize different aspects of solvation and to outline a possible computational strategy to describe dynamic and static effects due to bulk and specific peptide-solvent interactions.

1. Introduction

For a complete knowledge of the function of proteins and peptides, an understanding of the structure and dynamics of the environment, in general water, surrounding the biomolecule is essential. The water molecules that constitute the hydration shell in the immediate vicinity of the surface of proteins are particularly relevant to the function and, in that sense, are termed "biological water" as discussed by Nandi and Bagchi.[1] Now it is also known that the hydration shell surrounding a protein molecule comprises different types of water.[2] Few water molecules remain tightly bound to the protein for a very long time, whereas there are other water molecules still in the immediate vicinity of the surface of the protein that experience a much faster rotational and translational diffusion rate. Thus, biological water is believed to consist of two kinds of water molecules, usually referred to as bound and free, depending on their persistence on a given environment/binding site. There is, of course, dynamic exchange between the two species. The nature of this shell layer has been the focus of numerous both theoretical and experimental studies (see refs 3−10).

Among the various spectroscopic techniques used to understand the interaction of water with proteins, nuclear magnetic resonance spectroscopy (NMR) is one of the most extensively exploited. In particular, high-resolution NMR spectroscopy is used to determine the location of hydration water molecules in the interior and on the surfaces of proteins as well as their residence times.[11,12] The latter can be measured by two complementary NMR methods. One method measures intermolecular nuclear Overhauser effects (NOEs) between water protons and biomolecule protons, whereas the other records the nuclear magnetic relaxation dispersion (NMRD) of the quadrupolar water nuclei ^{17}O and ^{2}H. Also more standard NMR spectroscopy applications have long been used to study hydrogen bonding interactions, and more generally, solvation effects. In particular, $^{14}N/^{15}N$ and ^{17}O chemical shifts have been recognized to be very sensitive to micro environment of the nuclei and they are thus used as structural probes in peptides.

Besides this large, and increasing, experimental literature on the subject, there is no generalized picture of the nature and the dynamics of solvation of proteins and peptides at the local molecular level. Of course an accurate, possibly quantum-mechanical (QM), analysis of solvation on large systems like proteins and peptides is still an impossible task, and thus large simplifications or reductions have to be introduced. A common simplification is to shift from peptides to smaller model systems such as amides. However, also in this simplified subdomain, not so many examples of detailed theoretical studies have appeared so far, particularly if solvent effects are taken into account.

In the literature, there are three important theoretical investigations on solvent effects on ^{17}O and ^{15}N chemical shifts in amides. The oldest is due to Fiat and co-workers,[13] who suggested a model for separating the nuclear shielding constants due to hydrogen bonding-hydration phenomena at various sites in the amide molecule. In the second by Gerothanassis and Vakka,[14] an improved solvation model of amides based on ^{17}O NMR chemical shifts was presented: long-range dipole−dipole interactions, specific hydration at the amide oxygen, and cooperativity in hydrogen bonding of the bound molecules of water were indicated as important contributions in the overall chemical shift change between an amide oxygen in a vacuum and that which is fully hydrated in aqueous solution. In the third paper,[15] the model by Gerothanassis and Vakka was used in a more quantitative way by introducing a multiple-linear-regres-

* To whom correspondence should be addressed. E-mail: bene@dcci.unipi.it.
† Università di Pisa.
‡ Universidad de Sevilla.

10.1021/jp050035r CCC: $30.25
Published on Web 04/12/2005

sion analysis based on the Kamlet−Abboud−Taft solvatochromic parameters.[16] In all cases, the analyses were based on empirical (or semiempirical) methods.

In the following sections, we present the first quantum-mechanical analysis of solvent effects on oxygen and nitrogen shieldings in the simplest model generally used to represent the peptide function, namely *N*-methyl acetamide (NMA). This study is focused on NMA in water and acetone and it uses different solvation models involving either mean-field (or bulk) solvent effects (using the integral equation formalism, IEF,[17] polarizable continuum model, PCM[18]), or hydrogen bonding effects (through a supermolecule approach) or both (through a combined supermolecule/continuum approach). NMA-solvent supermolecules will be obtained either through QM geometry optimizations or molecular dynamics (MD) simulations. In all of the models, the solvent effects are included both in the geometry and in the calculation of the property at the density functional level of calculation.

This paper represents the second part of a study on the best strategy to describe solvation of peptides through computational approaches. In the first part[19] (from now on indicated as paper 1) the analysis was focused on IR and UV spectra of NMA in gas-phase and in water solution. The results of that analysis are here combined with the present one on NMR properties to get a more complete molecular picture of both static and dynamics aspects of solvation of peptides. In particular, by comparing results obtained with different, and in some way, complementary, computational approaches to experimental data obtained from techniques involving very different spectroscopic time-scales a clear view of limits and potentialities of the various solvation models can be appreciated.

2. Computational Details

Geometry optimizations for all of the systems (NMA and NMA-solvent clusters) both in vacuo and with IEF were performed at the density functional theory (DFT) level using the hybrid functional which mixes the Lee, Yang, and Parr functional for the correlation part and Becke's three-parameter functional for the exchange (B3LYP).[20] The basis set used was the 6-31+G(d,p).

In the IEF−PCM model, the molecular cavity is obtained in terms of interlocking spheres centered on selected nuclei. The chosen radii are 1.7 Å for carbonyl carbon, 2.0 Å for the methyl group, 1.6 Å for N, 1.52 Å for O, and 1.2 Å for H of H-bonded water.[21] All of the radii have been multiplied by a factor (equal to 1.2 if not otherwise specified) in order to take into account the fact that atomic bond or lone pair centers of the solvent molecules are normally located a bit further from the solute atoms than a van der Waals radius.[22] For all of the solvents, it is necessary to define the macroscopic permittivity; the values used in the following calculations are 78.39 for water and 20.70 for acetone.

Calculations of nuclear shieldings were performed at B3LYP level exploiting the gauge-including atomic orbitals (GIAO)[23] approach. The calculations on QM structures were performed at B3LYP/6-311+G(d,p), whereas those on MD structures were obtained exploiting a mixed basis set: 6-311+G(d,p) for the NMA molecule and 6-31G for the solvent molecules (this scheme will be indicated as hybrid). IEF−PCM has been generalized to GIAO method so to include solvent perturbation operators in the coupled perturbed scheme required to compute nuclear shieldings; for more details on the formalism, see ref 24.

All QM calculations both in vacuo and in solution were performed using the Gaussian code.[25]

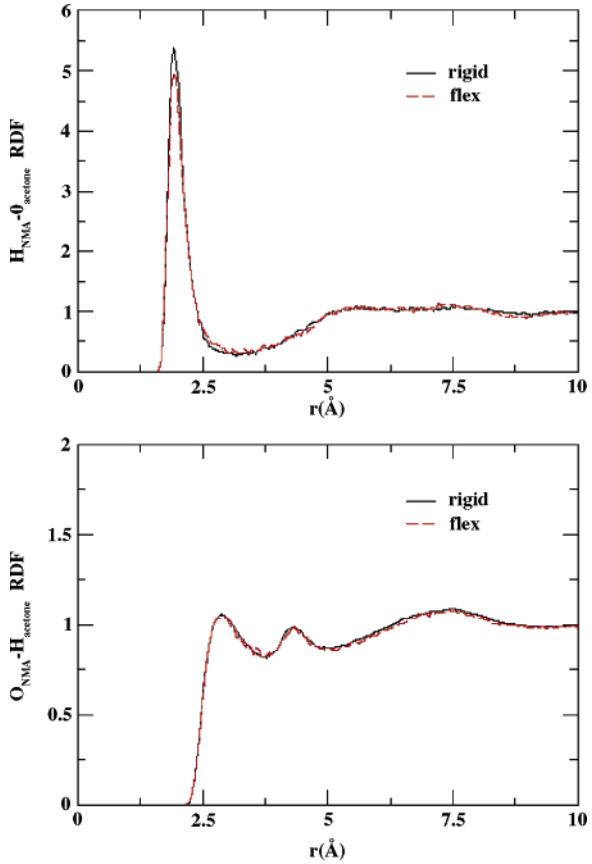

Figure 1. $H_{NMA}-O_{acetone}$ (top) and $O_{NMA}-H_{acetone}$ (botton) radial distribution functions for the rigid and flexible simulations (see text for details).

2.1. MD Simulations in Acetone. Simulations were performed in the NVE ensemble under periodic boundary conditions using the DL_POLY 2.13 package.[26] Simulation details of the aqueous NMA solution can be found in the preceding paper.[19] In the case of the acetone solution, a NMA molecule was immersed in an equilibrated box of 256 acetone molecules, where one solvent molecule was substituted by the NMA molecule. The final system reproduced the experimental solvent density[27] at 25 °C, 0.784 g/cm^3, by choosing the appropriate box side, $L = 31.56$ Å. The AMBER94 force field[28] parameters were chosen for the acetone description with the compatible set of charges derived by Jayaram et al.[29] Using rigid body equations of motion, the system was equilibrated at 300 K for 30 ps. Subsequently, production periods of 300 ps were obtained for two different simulations in which the solute was either rigid or flexible. Solvent molecules were considered rigid in both cases.

As in paper 1, also here information obtained from the radial distribution functions is used to select the sets of structures employed in the QM calculations (see also ref 30 for further details).

The first minima in $H_{NMA}-O_{acetone}$ and $O_{NMA}-H_{acetone}$ RDFs, Figure 1, are used as solvent cutoff distances. According to the integration numbers, about 3 solvent molecules solvate the C═O group, whereas in the N−H case, that figure is reduced by up to 1.2. As in the water case, the effect of using a flexible or rigid solute has only a marginal effect on the solvent distribution. It can be clearly seen from those plots that the solvent distribution is more tightly bound to the N−H group, where a well-defined H-bond is formed. The O_{NMA} and $H_{acetone}$ atoms are involved in a much weaker interaction, as clearly

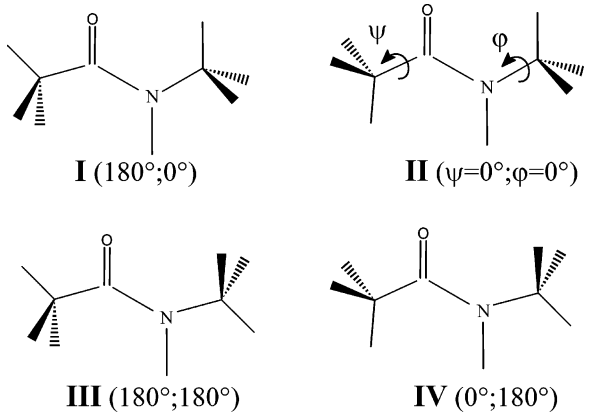

Figure 2. NMA conformers obtained by rotating the two methyl groups according to the angles ψ and φ.

reflected by the position (almost 1 Å longer) and value (1.1 vs 5.5) of the first maximum.

The strength of the solute−solvent interactions is also reflected in the dynamic properties of the solvent. Mean residence times[19,31] for the acetone molecules in the first solvation shell of the amide and carbonyl units have been computed. Values of 8 ± 0.5 ps and 2.5 ± 0.5 ps have been obtained for solvent molecules in the neighborhood of the N−H and C═O groups, respectively. This means that the persistence of the acetone molecules in the vicinity of the amide H atom is about 3−4 times longer than in the carbonyl group. Values have been obtained using the $O_{NMA}-C^{C=O}_{acetone}$ RDF information. If we use the $O_{NMA}-H_{acetone}$ RDF to compute the residence time of the methyl hydrogen atoms directly interacting with the NMA C═O unit, the value we get is even lower: 1.0 ± 0.3 ps, strengthening even more the differences between the carbonyl and amide solvation shells. These results differ from the ones obtained in the aqueous solutions where the persistence of water molecules around the C═O and N−H groups was similar, the first hydration shell of the carbonyl group presenting even slightly higher residence time values.

These results allow us to select the clusters to be used in QM calculations: acetone molecules having any O atom closer to the (N)H atom of NMA than the corresponding first minimum of the $(N)H_{NMA}-O_{acetone}$ RDF will be included in the cluster. An analogous criterion is applied for the $O_{NMA}-C^{C=O}_{acetone}$ pair. The selected structures were sampled at equal time intervals long enough (above 5 ps) so as to avoid correlation, so a proper sampling can be performed on the basis of the configurations used.

3. O and N Nuclear Shielding: Effect of Methyl Rotation

Following what reported in paper 1,[19] we have considered four different conformers of the *trans*-NMA molecule, each one characterized by a specific pair of values for the torsional angles φ and ψ. The four structures are reported in Figure 2 together with the values of the corresponding torsional angles φ and ψ.

The relative stabilities of the four conformers in gas-phase, acetone, and water (according to the continuum model) are reported in Table 1 together with the corresponding normalized Boltzmann weights (in parentheses). Gas-phase and water data have been extracted from paper 1 and they are reported here for clarity's sake.

Also in acetone, as in water, structures IV and I become the most and the least stable structures, respectively, inverting the gas-phase results. These results can be explained by considering that electrostatic effects due to polar solvents destabilize the structures with intramolecular interaction between oxygen lone pairs and the eclipsed H of the methyl group in favor of intermolecular interactions between solute polar groups and solvent. In any case the energy differences for each conformer in both solvents are very small, showing that at the continuum level both, water and acetone, behave very similarly.

TABLE 1: $\Delta G = G_X - G_{min}$ (kcal/mol) and normalized Boltzmann Weights of the Four Conformers (X = I, II, III, and IV) in the Gas Phase (vac) and in Two Solvents[a]

	vac	acet	water
I	0.98 (0.139)	1.79 (0.032)	1.87 (0.029)
II	0.00 (0.728)	0.82 (0.164)	0.87 (0.155)
III	2.06 (0.022)	0.86 (0.153)	0.92 (0.142)
IV	1.12 (0.111)	0.00 (0.651)	0.00 (0.675)

[a] Zero of energy is taken with respect to the most stable form in each phase.

TABLE 2: B3LYP/6-311+G(d,p) (GIAO) Oxygen and Nitrogen Nuclear Shieldings (in ppm) of the Four Conformers in the Gas Phase (vac) and in Two Solvents[a]

	vac		acet		water	
	σ(O)	σ(N)	σ(O)	σ(N)	σ(O)	σ(N)
I	−91.7	140.3	−41.8	132.2	−36.8	131.4
II	**−72.7**	**134.9**	−24.1	126.6	−19.6	125.8
III	−110.3	142.9	−58.0	134.0	−52.4	133.2
IV	−91.2	137.4	**−39.5**	**128.4**	**−36.1**	**127.7**

[a] Values in bold refer to absolute minima.

In Table 2, O and N isotropic nuclear shieldings are reported for each conformer in each phase. In bold, we indicate the values corresponding to the most stable conformer.

The effects of the two methyl rotations on the nuclear shieldings are important for both nuclei. More quantitatively, the largest differences among different conformers are found for gas-phase calculations where the variations with respect to the values corresponding to the stable conformer go up to 40 and 8 ppm for O and N shielding, respectively. As discussed in paper 1,[19] for isolated NMA, the relative energy of the various conformers, and thus the corresponding Boltzmann average of the nuclear shieldings, strongly depends on the QM level of calculation (for example, using B3LYP/6-31+G(d,p) factors, gas-phase averages are −78 ppm for O and 136 ppm for N, whereas if we use the MP2/6-311+G(d,p) factors reported in paper I, the averages change to −88 and 137 ppm, respectively). As a matter of fact, experiments[32] and calculations[33,34] seem to show that the torsional potential for ψ (HC3CN) and φ (CNC2H) for the isolated system is very flat, and the rotations can be considered as practically free at room temperature. This means that, within the NMR time scale of irradiation−absorption−detection ($\sim 10^{-3}$ s), the methyl groups undergo numerous rotations and thus what is observed is an averaged signal over all of these rotations. To compare with experimental data, we should thus consider all possible combinations of the two angles. As the rotations of the two methyl groups are not coupled, the strategy we have followed has been to calculate oxygen and nitrogen shieldings profiles with respect to each angle keeping fixed the other one, and then to arithmetically average along each profile: the resulting values are −91 ppm for O and 139 ppm for N. It is interesting to note that these values lie very close to those of conformer IV.

It has been shown that solvation effects, and in particular H bonds, increase the rotation barriers and that the stable conformation becomes that with $\psi = 0°$ and $\varphi = 180°$ (namely the conformer IV of Figure 2).[33] We note, however, that for solvated systems, the type of averaging is not as important as

for the isolated NMA: both B3LYP and MP2 Boltzmann averages as well as averages on all conformations lead to very similar values and close to those corresponding to the most stable conformer. For both solutions we can thus identify a single couple of average values: −39 ppm for O and 129 ppm for N in acetone and −36 ppm for O and 128 ppm for N in water.

Once the most appropriate treatment of the calculated data has been defined, the direct comparison with the experiments can be performed. Experimental data report an acetone-to-water shift of 60 ppm[14] for oxygen and −11 ppm[35] for nitrogen, but results shown in Table 2 lead, by far, to a smaller shift (only 4 ppm for O and −1 ppm for N). This discrepancy between computed and experimental shifts can be caused by an incomplete description of solvent effects obtained using the continuum-only model. However, it is not straightforward to say if this discrepancy comes from inaccuracies in the values calculated in water, in acetone, or in both. Unfortunately, no data are known for O and N shieldings in gas-phase or in apolar and aprotic solvents and thus no experimental gas-to-water or gas-to-acetone shifts are available. Nonetheless, an estimate from experimental data on similar systems can be done. In this sense, previous studies on dimethyl formamide (DMF)[14] have found a shift of 20 ppm for ^{17}O nuclear shielding passing from the apolar/aprotic *n*-hexane to acetone and 58 ppm for the acetone to water one. This latter value is very similar to that obtained for NMA and thus we can assume that also the *n*-hexane-to-acetone shift does not vary too much from DMF to NMA. In addition, if we assume that the shift from gas-to-*n*-hexane is at most a further small and positive value, we can estimate a lower limit of about 20 ppm for gas-to-acetone shift on NMA ^{17}O. For ^{15}N nucleus, the same kind of analysis leads to −10 ppm as an upper[35] limit for the gas-to-acetone shift.

By combining these estimates with the real experimental acetone-to-water shift, we can also give estimates for the gas-to-water shifts, namely (at least) 80 ppm for oxygen and (at most) −22 ppm for nitrogen. These estimates, even if not quantitative, suggest that the computed gas-to-water shifts are largely underestimated for both nuclei (if we consider the gas-phase averages values of −91 ppm for O and 139 ppm for N, we obtain shifts of 55 for O and −11 for N), whereas gas-to-acetone shifts are significantly overestimated for oxygen (the calculated shift is 52 ppm instead of 22 ppm) and slightly for nitrogen (−11 ppm instead of −10). Both of these effects go in the direction of reducing the computed acetone-to-water shifts which are in fact around 90% smaller than the experiments for both O and N nuclei.

The most straightforward way to improve the solvent model is to include possible specific solute−solvent effects (like those coming from H-bonds) by considering NMA-solvent clusters exactly as done in the previous analysis on vibrations and electronic transitions presented in paper 1.

4. Effect of H-Bonding on Nuclear Shieldings

4.1. Acetone. To get an accurate description of short-range specific effects induced by H-bonding, here we consider clusters formed by solute and few solvent molecules. The structure of clusters can be alternatively obtained through QM geometry optimizations and MD simulations.

According to what was reported in section 2.1, it follows that the strongest H-bond effects come from the interaction between the NMA (N)H atom and the acetone oxygen (see Figure 1). We have thus optimized the corresponding cluster (from now on indicated as Hb cluster) at the QM level (B3LYP/6-31+G(d,p)) with and without the IEF continuum. In Figure 3, we report the graphical representation of the Hb cluster obtained in gas phase and in the presence of the external continuum with the indication of the interaction distances. We note that NMA presents the same conformation in both VAC and IEF clusters, and this coincides with the previously indicated conformation IV.

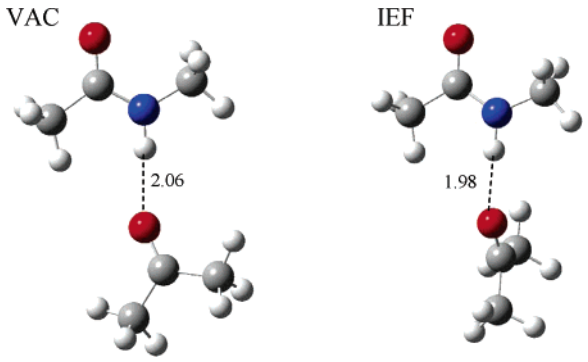

Figure 3. Structures of the NMA-acetone (Hb) clusters in gas phase (VAC) and in the presence of the external IEF continuum.

TABLE 3: B3LYP/6-311+G(d,p) (GIAO) Oxygen and Nitrogen Nuclear Shieldings (in ppm) of NMA-acetone Clusters in the Gas Phase (vac) and with the IEF[a]

	vac		IEF	
	σ(O)	σ(N)	σ(O)	σ(N)
Hb	−78.1	134.8	−31.4	124.9
$\langle rig_{NH} \rangle$	−87.1	132.8	−37.7	124.2
$\langle flex_{NH} \rangle$	−83.5	142.2	−35.3	133.9
$\langle rig \rangle$	−79.3	130.0	−67.1	127.1
$\langle flex \rangle$	−77.3	139.5	−64.2	136.2

[a] The row indicated as $\langle rig \rangle$ refers to average values on MD structures obtained with a rigid model. The rows indicated as "flex" refers to average values of MD structures obtained with a flexible model (see text for details). For all the MD structures an hybrid basis (6-311+G(d,p) for the NMA molecule and 6-31G for the acetone molecules) has been used.

A possible further interaction among NMA and acetone molecules is between methyl hydrogens of acetone and the carbonyl oxygen of NMA. However, this kind of interaction is too weak to be correctly described through a static picture as that represented by a QM optimized cluster, whereas it can be accounted for through averages on clusters obtained from MD runs.

For MD structures, two different types of clusters have thus been defined, namely those obtained including solvent molecules belonging to the first solvation shell around the (N)H, and the larger ones obtained combining the N(H) and (C)O solvation shells: see section 2.1 for more details. In addition, each type of clusters can be alternatively obtained from MD simulations performed using a rigid or a flexible model for NMA. To distinguish between the origin of the different sets of clusters, we shall use the labels "rig" and "flex" and the index "NH" to indicate the smaller clusters obtained only by considering the solvent molecules around the (N)H group. We also recall that, in the rigid model, the NMA structure is kept frozen in the IV-like structure obtained in the previous QM-IEF optimization, whereas in the flexible model, all internal degrees of freedom (including the rotation angles) can change. The computed isotropic shieldings for the different structures of each set (which are not reported) have been arithmetically averaged to give the values shown in Table 3. The average (here indicated by the $\langle\ \rangle$ symbol) is obtained for a set of 60 and 40 different clusters for the flexible and the rigid model, respectively.

Starting the analysis from the isolated Hb cluster, we find a very small change in O and N shieldings with respect to the values reported in Table 2 for the most stable conformer in the isolated NMA. This observation, however, has to be refined by noting that in this comparison two different effects have been combined. The Hb cluster presents in fact a IV-like structure and thus the correct values of Table 2 to compare with, to evaluate direct H-bonding effects (i.e., without the indirect effect of a different conformation in the NMA molecule) are those corresponding to the conformer IV, namely −91 ppm for O and 137 ppm for N. In this way, we get a net effect due to specific (N)H···O(acetone) interactions of 13 ppm for O and −3 ppm for N.

When we add the IEF continuum, the computed shieldings in the Hb cluster are −31 ppm for O and 125 ppm for N. Comparing these results with those obtained with the continuum only approach (see the center column of Table 2), it follows that including (N)H···O(acetone) H-bonding interactions does not improve the description. On the contrary, it slightly amplifies the overestimation of the solvent effects found with IEF only approach: the long-range electrostatic and H-bonding effects, coupled through a QM minimized structure, seem to act in the same direction. Finally, it is interesting to note how the N−H unit affects the electronic distribution in the amide C═O part, provoking a nonnegligible NMR shift for the ^{17}O signal as well.

In the analysis of the results coming from MD structures, where only the N(H) solvation shell is taken into account, we first note that for O rigid and flexible models give similar descriptions (both in the gas phase and with IEF). When compared to Hb results, we observe that MD clusters in the gas phase present a smaller shift (the difference with respect to NMA-IV is here 4 ppm for the rigid model and 8 ppm for the flexible one, whereas in the Hb cluster, it was 13 ppm). When we add the IEF continuum, the differences with respect to the Hb cluster significantly reduce, and practically, we do not observe any real improvement in the description of the gas-to-acetone shift with respect to the continuum-only model or the Hb cluster: also by introducing solvent molecules representing the solvation shell around the (N)H center, the carbonyl oxygen still remains too shielded.

It is interesting to compare these results with those obtained using larger MD clusters that include acetone molecules belonging to both (C)O and (N)H solvation shells (see section 2.1 for details). The new average value obtained on the parallel set of structures becomes −79.3 in the gas phase and −67.1 ppm when the IEF continuum is added. As can be seen comparing these values with the previously discussed ones, the addition of the (C)O solvation shell induces an important shift in the oxygen nuclear shielding, namely 8 ppm in the gas phase and 29 ppm with the continuum. This is indeed an interesting result as now the net gas-to-acetone shift reduces to 24 ppm instead of the 50−60 ppm observed for the smaller MD clusters, the QM Hb, and the continuum-only model. This important reduction of the shift, which now becomes very close to the experimental estimate of ∼20 ppm, seems to indicate that solvation around (C)O involves a cage of acetone molecules preferentially oriented with their methyl groups pointing toward the NMA oxygen and thus preventing a close contact between NMA and acetone.

A first confirmation of this analysis is given by the RDF reported in section 2.1 to which we can add here some further comments. As done in paper 1, to study the hydration structure around the NMA molecule, we introduce here a spatial distribution function 3-D picture representing the distribution

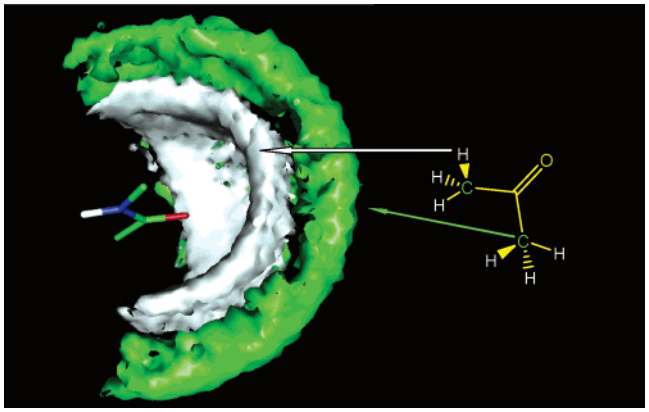

Figure 4. Acetone methyl carbon (green) and hydrogen (white) spatial distribution functions around NMA carbonyl oxygen contoured at 75% above bulk density.

adopted by the acetone molecules around the O(C) of NMA. The SDF, we recall, is defined by isovalue surfaces, and it shows the highest probability regions for finding a given type of atom in the neighborhood of a site of interest. In Figure 4, the higher acetone methyl carbon and hydrogen density regions around the amide group can be observed.

The relevance of the presence of solvent molecules in the neighborhood of the carbonyl group could be obvious in the case of water, where the C═O group interacts with the solvent by means of H bonds, whereas in acetone the interaction between the carbonyl group and the methyl hydrogens is much weaker. However, the explicit solvent presence implies that long-range effects introduced by the continuum model must be taken into account at much longer distances than the usual $1.2r_{vdW}$ used to define the sphere around each solute atom. Otherwise, an excessive oxygen polarization is induced by the solvent. A check can be done recomputing the oxygen nuclear shielding using a cavity with larger radii for the sphere centered on the oxygen atom. By changing the scaling factor of the radius of the oxygen sphere (leaving fixed those of the other spheres) from 1.2 (i.e., the value used to get results of Table 2) to 1.3, 1.4, and 1.5, we find a change in the nuclear shielding of −12, −17, and −22. It means a final gas-to-water shift of 40, 35, and 30 ppm, respectively, in comparison to the 52 ppm found with the standard cavity.

Passing now to N shielding, the first important thing to observe is that, this time, rigid and flexible values are quite different. Rigid values go in the direction to reduce the shielding with respect to the isolated NMA as expected, and they give results very similar to Hb clusters both in gas-phase and with the IEF continuum. On the contrary, the flexible results increase such value if calculated in the gas phase, or they leave it almost unchanged if calculated with IEF.

The differences between rigid and flexible models can be imputed to geometrical effects; in fact, whereas in the rigid model the NMA geometry is kept fixed in the structure obtained in the QM-IEF optimization, in the flexible model, each NMA−acetone cluster presents a different geometry for NMA. As nuclear shieldings are extremely sensitive to geometrical changes, it becomes important to try to quantify such effect.

To check geometry effects, we have recomputed O and N shieldings at B3LYP/6-311+G(d,p) for NMA by using the geometries resulting from the various QM and MD clusters. By comparing the results of these calculations with those reported in Table 2 for NMA-IV conformer, we can quantify the effects due to changes in geometry passing from single NMA to clusters. The results are reported in Table 4. For a more direct

TABLE 4: O and N Nuclear Shieldings (in ppm) of NMA in the Gas Phase (vac) and with the IEF Continuum[a]

	vac		IEF	
geom	σ(O)	σ(N)	σ(O)	σ(N)
NMAIV	−91.3	137.4	−39.5	128.4
Hb	−85.2	138.3	−35.5	129.4
⟨flex⟩	−91.9	145.4	−39.1	137.1

[a] Geometries of NMA are extracted from NMA−acetone clusters.

comparison, in the table, we also report the values obtained for the NMA-IV conformers already presented in Table 2 (we do not report results referring to the rigid system as these coincide with NMA-IV values).

From data of Table 4, it is evident that geometry effects are much more important for N than for O. In particular, it has to be observed that flexible MD results cannot be taken as completely reliable for N shielding. An analysis on the geometrical differences between the structure obtained as an average on all of the flexible MD configurations and the QM structure has shown that the "unexpected" values of nitrogen nuclear shieldings when computed on the flex structures are due to a larger (O)C−N bond length. The average C−N value in the MD simulation is 1.338 Å, smaller than the 1.352 Å value obtained in the QM geometry optimization including the continuum. This high sensitivity of NMR chemical shifts to bond lengths has already been observed[36] for some nuclei.

4.2. Water. Exactly as done for acetone solution also for water, to get a more accurate description of solvent effects on nuclear shieldings, we consider clusters formed by solute and some solvent molecules. The details of the geometries of these clusters, see Figure 5, together with their vibrational and electronic analysis are reported in paper 1.

In Table 5, we report the shieldings for all of the three sets of clusters described in the previous section in gas and with the IEF continuum.

The results clearly show the high sensitivity of the carbonylic oxygen to the environment: this is not surprising because this oxygen is dominated by the paramagnetic part. We recall that paramagnetic shielding, which arises from the nonspherical orbitals, is associated with the orbital angular momentum of electrons and is therefore dependent on excited states of the molecule. Paramagnetic contributions normally result in deshielding and are the terms mostly affected by solvation effects and

TABLE 5: B3LYP/6-311+G(d,p) (GIAO) Oxygen and Nitrogen Nuclear Shieldings (in ppm) on H-Bonded Clusters in the Gas Phase (vac) and with the IEF Continuum[a]

	σ(O)		σ(N)	
	vac	IEF	vac	IEF
+1wOL	−63.4	−22.7	134.5	125.2
+1wOR	−60.8	−21.5	131.4	124.8
+1wN	−84.9	−31.1	133.8	122.7
+2wOO	−36.2	−7.6	128.0	121.7
+2wONL	−57.0	−17.7	130.5	120.3
+2wONR	−54.2	−16.5	127.7	119.6
+3w	−29.7	−3.9	124.0	116.5

[a] The geometries of the clusters have been obtained at B3LYP/6-31+G(d,p) and they are all of type (IV).

in particular H bonds. An approximate but effective interpretation of the (local) paramagnetic contribution in terms of electronic properties has been originally formulated by Pople.[37] According to this model, variations in nuclear shielding of an atom can be related to changes in its local charge densities, bond orders, and energies of electronically excited states. If we apply this scheme to the interpretation of solvent effects on O, the attention has to be focused on lone pair orbitals. When the molecule is isolated, a π-electron system is available for low-energy $n \rightarrow \pi^*$ transitions, and a large (negative) paramagnetic term will be found. In contrast, the destabilizing effects of the $n \rightarrow \pi^*$ state due to interactions with a polar solvent (i.e., the blue shift discussed in paper 1) and/or an H-bond will reduce its contribution and, as a consequence, the absolute magnitude of the paramagnetic term. As a final result, the total nuclear shielding will be less negative. This is exactly what happens to the NMA oxygen passing from isolated to IEF clusters on one hand and from 1wN to 2wON and 2wOO clusters, on the other hand.

Let us now consider structures derived from MD snapshots taken at different simulation times.

As for NMA−acetone clusters, also here the calculations on MD clusters have been obtained with the same hybrid basis set (6-311+G(d,p) for the NMA molecule, and 6-31G for the water molecules). Oxygen and nitrogen shieldings obtained from these calculations are reported in Table 6. The data are divided into two groups depending on the type of model used in the MD simulation, namely a rigid and a flexible one (see section 2.1 for details). The O and N nuclear shieldings obtained for each

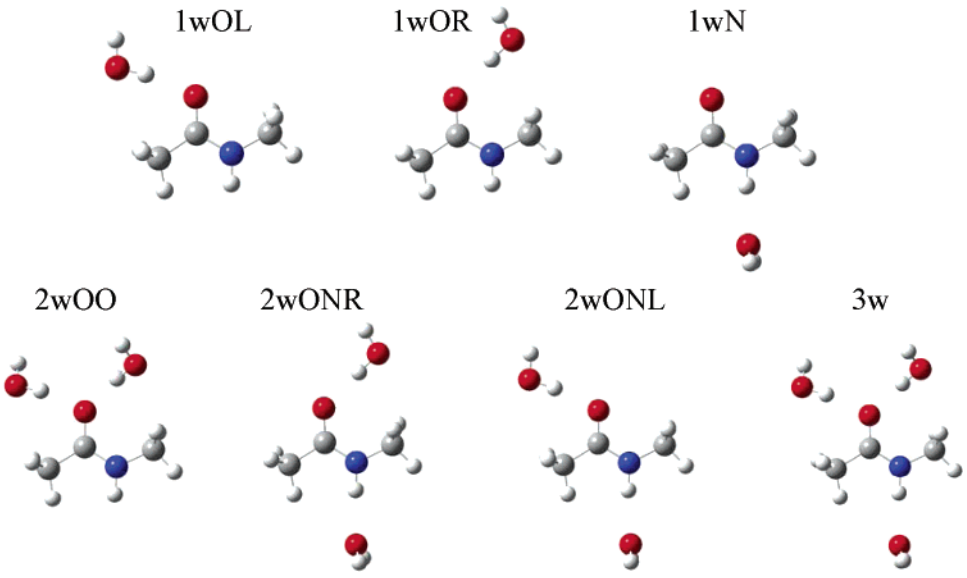

Figure 5. Schematic picture of the structures of the NMA-nw clusters with indication of the corresponding labels.

TABLE 6: B3LYP (GIAO) Oxygen and Nitrogen Nuclear Shieldings (in ppm) Computed on MD Clusters in the Gas Phase (vac) and with the IEF Continuum Using an Hybrid Basis (6-311+G(d,p) for the NMA Molecule and 6-31G for the Water Molecules)

	σ(O)		σ(N)	
	vac	IEF	vac	IEF
⟨rig⟩	−47.2	−17.8	124.5	118.3
⟨flex⟩	−45.6	−15.2	131.1	124.8

different structure with and without adding an external continuum have been arithmetically averaged to yield the values reported in Table 6 (the average is on a set of 60 and 40 different clusters for the flexible and the rigid model, respectively).

We note that for oxygen, the two alternative MD models, i.e., the flexible and the rigid one, give very similar results (both for gas-phase and for IEF scheme), whereas the results obtained for nitrogen differ significantly. This difference between the two models can be explained exactly in the same way as previously done for acetone (see section 4.1 and Table 4). Also here, the results obtained using the structures of NMA resulting from QM and MD-flex structures show that the latter present an unexpected behavior for N shieldings due to the differences in the geometrical parameters, especially the (O)C−N bond length. Due to this limitation, in the following analysis, results from flexible MD will not be considered anymore.

5. Discussion

The results reported in the previous section are better analyzed in terms of shifts on O and N shieldings and how they compare with experiments.

In section 3, we have presented and discussed the problems due to the fact that, to the best of our knowledge, the only experimental data available refer to acetone-to-water shifts. There we have also described the strategy we have followed to overcome these problems and find a reliable estimate of gas-to-solvent shifts for both acetone and water exploiting experimental data on similar systems and combining them with the available acetone-to-water shifts. Following this strategy, for gas-to-acetone shifts, a lower limit of 20 ppm for oxygen and an upper limit of −10 ppm for nitrogen has been defined whereas for gas-to-water shifts the estimates are 80 ppm for oxygen and −21 ppm for nitrogen. Using these values as reverences we have thus compared the different models used for both solvents obtaining the following results.

Acetone. In Figure 6, the gas-phase values are those obtained assuming a free rotation of both methyl groups (see section 3), and the experimental estimates are reported as dotted lines.

For oxygen, the values reported in Figure 6 indicate that the long-range mean-field (or continuum) description alone overestimates the observed solvent effect on O shielding. If we try to include short-range effects on (N)H, either through a single H-bonded molecule (Hb) or through an average on MD structures including only (N)H solvation shell(s) (⟨rig$_{NH}$⟩) we do not really improve the description. The results becomes significantly better if we consider clusters including also the (C)O solvation shell (⟨rig⟩). It thus appears important to consider that short-range interactions of methyl groups with NMA carbonyl oxygen create a sort of cage around it which prevents the polar part of the solvent molecules to be in close contact to the solute. This phenomenon has been pointed out in section 4.1 where we have shown that a rather homogeneous sphere-like distribution protects the C═O group from direct interactions with the polar carbonyl group of the acetone molecule (see Figure 4).

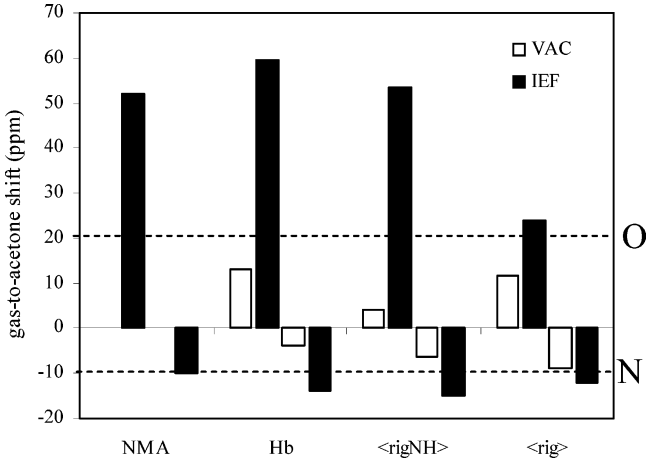

Figure 6. Gas-to-acetone shifts for O and N using various descriptions: a continuum only model (NMA), QM hydrogen-bonded clusters (Hb), and two different sets of MD-clusters, one set obtained including solvent molecules belonging to the first solvation shell around the (N)H (⟨rig$_{NH}$⟩), and the second obtained combining the N(H) and (C)O solvation shells (⟨rig⟩). Each set of clusters has been studied in gas-phase (VAC) or with an external continuum (IEF). Experimental estimates are reported as dotted lines.

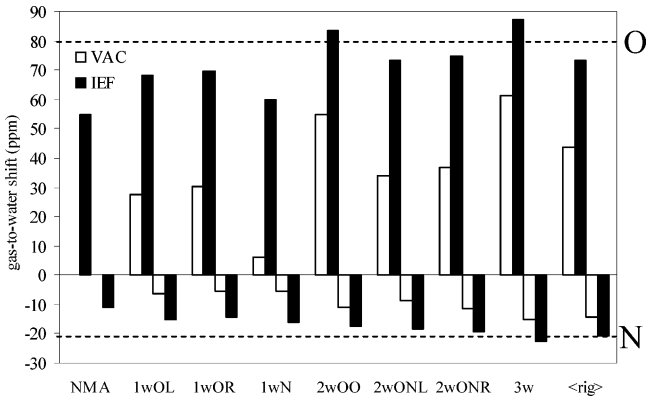

Figure 7. Gas-to-water shifts for O and N using various descriptions: a continuum only model (NMA), QM Hydrgen-bonded clusters (nwXY, with X,Y═O,N and n = 1,2,3) and MD-clusters (⟨rig⟩). Each set of clusters has been studied in the gas phase (VAC) or with an external continuum (IEF). Experimental estimates are reported as dotted lines.

For nitrogen, the analysis seems less complex than for oxygen; in fact, in this case, the continuum-only model gives a reasonably correct description as shown by the first point on the left of the graph reported in Figure 6. As a matter of fact, for nitrogen, solvent effects are much lower than for oxygen and thus the range of variability of the various models (continuum, QM Hb cluster, or MD clusters) is limited. In any case, we can observe that once again it is important to correctly describe solvation around the whole molecule (i.e., not only around the nucleus of interest) and thus clusters including also the (C)O solvation shell (⟨rig⟩) give better results than those accounting for NH solvation only (Hb and ⟨rig$_{NH}$⟩). Finally it is worth mentioning that the addition of an external continuum always improves the descriptions (see the comparison between "vac" and "IEF" points).

Water. Following a similar strategy, results obtained with the different solvation models are reported in Figure 7.

Once again the graphs show the fundamental role acted by mean-field (or continuum) interactions: all of the clusters (either QM or MD) when described in the gas phase account only for a part of the "observed" shift on both O and N nuclei. Also in the case of a complete saturation of all H-bonding sites (as in

3w cluster), it appears that an important part of solvation is still missing. This part is recovered by introducing the additional long-range continuum effect. This result is not unexpected after the analysis on IR and UV spectra reported in paper 1. Here, however, a further aspect can be introduced. The comparison of gas-phase and IEF results on one hand and QM and MD results (both including IEF) on the other hand shows that hydration of NMA is better represented in terms of two types of waters: a more mobile (or free) water whose effects are properly accounted for by a mean-field description, and a more static (or rigid) water which on the contrary has to be explicitly described at an accurate molecular level.

This latter type of water, however, is not exactly represented by a single cluster in which all possible H-bonding interactions are accounted for (namely 3w). In this way, in fact, we introduce an excessive rigidity in the hydration structure at the NMA surface and the shift we compute for both shieldings is too large (we note that the estimate of 80 for oxygen shift is an upper limit and the 3w is above this limit). Obviously when passing from the 3w to the 2wOO cluster (i.e., eliminating the direct H-bonding on H(N)) we still observe a similar overestimation on oxygen, whereas on N, we now find a too small effect. The mixed 2wONR shows a good behavior for both nuclei (with a small underestimation on O which however well correlates with the guess of the real shift which should be a bit smaller than 80). Nonetheless, the most correct behavior is however presented by the average values on MD clusters: for both nuclei, in fact, the correlation with experiments is very good, This fact shows, once more, that a correct description of solvent effects is correctly obtained by including dynamic effects on solvation shells through averages on different clusters (of various size) generated by a statistical method like MD. In this way, fluctuations in the number of solvent molecules and in their positions are explicitly described.

6. Conclusions

To understand the solvation (and, more specifically, hydration) of peptides at the molecular scale, several questions need to be addressed: What are the time scales for solvent relaxation in the immediate vicinity of a peptide surface? Are there local rigid structures of solvent at the surface, and how uniform is the protein surface? How does solvation at the surface differ from that of bulk solvent?

In this paper and in the related one,[19] we have proposed a computational strategy to try to answer these fundamental questions. This strategy is based on an important simplification, which becomes compulsory anytime an accurate QM analysis is required, namely that of resorting to a model system (NMA) to represent the basic functions of peptides instead of considering the real system. NMA is then used to study how the main spectroscopic properties characterizing peptides are modified by solvation. As the main interest in peptides is for hydration, the largest part of the study has been devoted to water as solvent, but to distinguish between H-bonding effects and polarization effects, we have considered a second, still polar but nonprotic solvent, namely acetone.

The use of spectroscopic properties to probe solvation effects is not new; here however, a different approach is followed: the comparison of experimental and calculated properties related to spectroscopies involving very different times of measure (NMR on one hand, and IR and UV on the other hand) is here exploited to define limits and potentialities of different solvation models to describe static and dynamic aspects of solvation. In particular, the step-by-step strategy used has involved QM and classical simulations to determine the geometrical structures of NMA and NMA−solvent clusters and QM (namely DFT) methods to estimate the NMR (in the present paper) and the IR and UV (in paper 1) properties of isolated and solvated NMA described through a continuum, a discrete, and a mixed continuum/discrete solvation model.

In short, the theoretical studies performed in these two works have shown the need of an appropriate consideration of the specific effects of those solvent molecules directly interacting with the solute moieties under study. It is important to notice that this need is revealed independently of the strength of the solute−solvent interaction. For example, the presence of solvent molecules in the neighborhood of the carbonyl group is crucial to understand the observed chemical shifts on both nuclei even in polar and nonprotic solvents such as acetone. Although it could be obvious in the case of water, where the (C)O directly interacts with the solvent by means of strong H bonds, it is not so in acetone, where the interactions between the carbonyl group and the methyl hydrogens are much weaker. However, also in the latter case we have shown that the presence of explicit solvent molecules is compulsory, otherwise, an excessive oxygen polarization is induced by the solvent if a continuum only model is used. A possible explanation of this finding is in terms of nonelectrostatic (or van der Waals) effects which are not included in the continuum approach used here. A similar behavior has been already observed for nitrogen nuclear shieldings in pyridine and diazines.[38]

In addition, we have shown that, if a quantitative agreement with experimentally observed solvent induced shifts is intended, then the long range solvent effects are always crucial. Even more, the explicitly considered solvent molecules must contain the statistical information present in the nature of the solute−solvent interactions in solution. This can be easily introduced by means of classical MD simulations using appropriate force fields whereas the long-range mean-field effects can be properly taken into account by means of the PCM model that becomes an extremely efficient alternative to larger solvent clusters.

In this work devoted to NMR, we have also shown that classical force fields may exhibit significant limitations. Although for the UV spectroscopy[19] the simulation results obtained using a rigid or flexible solute are similar, this is no longer true for nuclear shieldings (especially for N nucleus): even small geometry distortions can give rise to large effects on the property. Such a limitation can be easily overcome by using QM based solute geometries, although, it is important to remark that in order to make the statistical ensemble generated by the simulation appropriate to compute this kind of property, a careful analysis of geometrical differences between the QM geometry and those resulting from MD snapshots has to be done. The use of more sophisticated (and much more CPU expensive) strategies, like ab initio MD simulations obviously are not affected by this difficulty. However, then, the reliability of the results resides on the ability of the quantum chemistry level of computation, in most of the applications based on DFT, to properly describe solute−solvent and solvent−solvent interactions where van der Waals type of forces can be crucial for a proper structural and dynamic phase space sampling.[39] Needless to say that, also, the simulation time becomes a crucial parameter for a proper solvent configurational sampling: a key factor, according to the results obtained in these two papers, for reliable spectroscopic estimations. In this sense, the mean residence times obtained by means of classical MD simulations could be used as reference values for lower limits of simulation times in more sophisticated ab initio simulations.

In conclusion, it can be noted that all of the results of this articulated study on different properties should be used to better appreciate the drawbacks of the different levels of sophistication based on QM or QM and MM mixed strategies usually considered to mimic solvent as well to better understand static and dynamic aspects of solvation. Both these pieces of information become in fact of fundamental importance when dealing with larger and much more computationally expensive systems where the cheaper alternatives not only become attractive but, often, also necessary.

Acknowledgment. J.M.M. thanks Junta de Andalucía and Spanish DGICYT (BQU2002-02217) for financial support.

References and Notes

(1) Nandi, N.; Bagchi, B. *J. Phys. Chem. B* **1997**, *101*, 10954.
(2) Gregory, R. *Protein−Solvent Interactions*; Dekker: New York, 1995.
(3) Burling, F.; Weis, W.; Flaherty, K.; Brunger, A. *Science* **1996**, *271*, 72.
(4) Svergun, D.; Richard, S.; Koch, M.; Sayers, Z.; Kuprin, S.; Zaccai, G. *Proc. Natl. Acad. Sci. U.S.A.* **1998**, *95*, 2267.
(5) Makarov, V.; Feig, M.; Andrews, B. K.; Pettitt, B. M. *Biophys. J.* **1998**, *75*, 150.
(6) Teeter, M. *Annu. Rev. Biophys. Biophys. Chem.* **1991**, *20*, 577.
(7) Phillips, G.; Pettitt, B. M. *Protein Sci.* **1995**, *4*, 149.
(8) Pal, S.; Peon, J.; Zewail, A. *Proc. Natl. Acad. Sci.* **2002**, *99*, 1763.
(9) Beveridge, D.; Swaminathan, S.; Ravishanker, G.; Withka, J. M.; Srinivasan, J.; Prevost, C.; Louise-May, S.; Langley, D. R.; DiCapua, F. M.; Bolton, P. H. In *Water and Biological Macromolecules*; Westhof, E., Ed.; CRC Press: Boca Raton, FL, 1993.
(10) Despa, F.; Fernandez, A.; Berry, R. S. *Phys. Rev. Lett.* **2004**, *93*, 228104.
(11) Otting, G.; Liepinsh, E. *Acc. Chem. Res.* **1995**, *28*, 171.
(12) Halle, B.; Denisov, V. P.; K., V. In *In Biological Magnetic Resonance, Vol. 17: Structure Computation and Dynamics in Protein NMR*; Krishna, N. R., Berliner, L. J., Eds.; Kluwer Academic/Plenum Press: New York, 1999; p 419.
(13) Burgar, M.; Amour., T. S.; Fiat, D. *J. Phys. Chem.* **1981**, *85*, 502.
(14) Gerothanassis, I. P.; Vakka, C. *J. Org. Chem.* **1994**, *59*, 2341.
(15) Díez, E.; Fabián, J. S.; Gerothanassis, I.; Esteban, A.; Abboud, J.-L. M.; Contreras, R.; de Kowalewski, D. *J. Magn. Reson.* **1997**, *124*, 8.
(16) (a) Kamlet, M. J.; Abboud, J.-L. M.; Taft, R. W. *Prog. Phys. Org. Chem.* **1981**, *13*, 485. (b) Kamlet, M. J.; Abboud, J.-L. M.; Abraham, M. H.; Taft, R. W. *J. Org. Chem.* **1983**, *48*, 2877. (c) Abraham, M. H.; Grellier, P. L.; Abboud, J.-L. M.; Doherty, R. M.; Taft, R. W. *Can. J. Chem.* **1988**, *66*, 2673.
(17) (a) Cancés, E.; Mennucci, B. *J. Math. Chem.* **1998**, *23*, 309. (b) Cancés, E.; Mennucci, B.; Tomasi, J. *J. Chem. Phys.* **1997**, *107*, 3031. (c) Mennucci, B.; Cancés, E.; Tomasi, J. *J. Phys. Chem. B* **1997**, *101*, 10506.
(18) (a) Miertus, S.; Scrocco, E.; Tomasi, *J. Chem. Phys.* **1981**, *55*, 117. (b) Cammi, R.; Tomasi, J. *J. Comput. Chem.* **1995**, *16*, 1449.
(19) Mennucci, B.; Martínez, J. M. *J. Phys. Chem. B* **2005**, *109*, 9818.
(20) (a) Becke, A. D. *J. Chem. Phys.* **1993**, *98*, 5648. (b) Lee, C.; Yang, W.; Parr, R. G. *Phys. Rev. B* **1988**, *37*, 785.
(21) Bondi, A. *J. Phys. Chem.* **1964**, *68*, 441.
(22) Tomasi, J.; Persico, M. *Chem. Rev.* **1994**, *94*, 2027.
(23) Hameka, H. *Rev. Mod. Phys.* **1962**, *34*, 87. (b) Ditchfield, R. *Mol. Phys.* **1974**, *27*, 789. (c) Wolinski, K.; Hinton, J.; Pulay, P. *J. Am. Chem. Soc.* **1990**, *112*, 8251.
(24) (a) Cammi, R. *J. Chem. Phys.* **1998**, *109*, 3185. (b) Cammi, R.; Mennucci, B.; Tomasi, J. *J. Chem. Phys.* **1999**, *110*, 7627.
(25) Frisch, M. J.; Trucks, G. W.; Schlegel, H. B.; Scuseria, G. E.; Robb, M. A.; Cheeseman, J. R.; Montgomery, J. A., Jr.; Vreven, T.; Kudin, K. N.; Burant, J. C.; Millam, J. M.; Iyengar, S. S.; Tomasi, J.; Barone, V.; Mennucci, B.; Cossi, M.; Scalmani, G.; Rega, N.; Petersson, G. A.; Nakatsuji, H.; Hada, M.; Ehara, M.; Toyota, K.; Fukuda, R.; Hasegawa, J.; Ishida, M.; Nakajima, T.; Honda, Y.; Kitao, O.; Nakai, H.; Klene, M.; Li, X.; Knox, J. E.; Hratchian, H. P.; Cross, J. B.; Adamo, C.; Jaramillo, J.; Gomperts, R.; Stratmann, R. E.; Yazyev, O.; Austin, A. J.; Cammi, R.; Pomelli, C.; Ochterski, J. W.; Ayala, P. Y.; Morokuma, K.; Voth, G. A.; Salvador, P.; Dannenberg, J. J.; Zakrzewski, V. G.; Dapprich, S.; Daniels, A. D.; Strain, M. C.; Farkas, O.; Malick, D. K.; Rabuck, A. D.; Raghavachari, K.; Foresman, J. B.; Ortiz, J. V.; Cui, Q.; Baboul, A. G.; Clifford, S.; Cioslowski, J.; Stefanov, B. B.; Liu, G.; Liashenko, A.; Piskorz, P.; Komaromi, I.; Martin, R. L.; Fox, D. J.; Keith, T.; Al-Laham, M. A.; Peng, C. Y.; Nanayakkara, A.; Challacombe, M.; Gill, P. M. W.; Johnson, B.; Chen, W.; Wong, M. W.; Gonzalez, C.; Pople, J. A. *Gaussian 03*, revision A.1; Gaussian, Inc.: Pittsburgh, PA, 2003.
(26) Smith, W.; Leslie, M.; Forester, T. R. *CCLRC*; Daresbury Laboratory: Daresbury, Warrington, U.K.
(27) Riddick, J. A.; Bunger, W. B.; Sakano, T. K. *Techniques of Chemistry, Vol. II: Organic Solvents, Physical Properties and Methods of Purification*; Wiley: New York, 1986.
(28) Cornell, W. D.; Cieplak, P.; Bayly, C. Y.; Gould, I. R.; Merz, K. M., Jr.; Ferguson, D. M.; Spellmeyer, D. C.; Fox, T.; Caldwell, J. W.; Kollman, P. A. *J. Am. Chem. Soc.* **1995**, *117*, 5179.
(29) Jayaram, B.; Sprous, D.; Beveridge, D. L. *J. Phys. Chem. B* **1998**, *102*, 9571.
(30) Mennucci, B.; Martínez, J. M.; Tomasi, J. *J. Phys. Chem. A* **2001**, *105*, 7287.
(31) Values obtained with $t^* = 0$. See ref 19 for further details.
(32) Ohashi, N.; Hougen, J. T.; Suenram, R. D.; Lovas, F. J.; Kawashima, Y.; Fujitake, M.; Pyka, J. *J. Mol. Spectrosc.* **2004**, *227*, 28.
(33) Guo, H.; Karplus, M. *J. Phys. Chem.* **1992**, *96*, 7273.
(34) Villani, V.; Alagona, G.; Ghio, C. *Mol. Eng.* **1999**, *8*, 135.
(35) Witanowski, M.; Stefaniak, L.; Webb, G. *Annual Reports on NMR Spectroscopy*; Academic Press: London, 1993; Vol. 25.
(36) Oldfield, E. *Annu. Rev. Phys. Chem.* **2002**, *53*, 349.
(37) Pople, J. A. *Discuss. Faraday Soc.* **1962**, *34*, 7.
(38) Mennucci, B. *J. Am. Chem. Soc.* **2002**, *124*, 1515.
(39) Milet, A.; Korona, T.; Moszynski, R.; Kochanski, E. *J. Chem. Phys.* **1999**, *111*, 7727.